IEEE Photonics Journal
An IEEE Photonics Society Publication

Open Access

Resonances in Bianisotropic Layers

Volume 10, Number 1, February 2018

Faroq Razzaz
Majeed A. S. Alkanhal

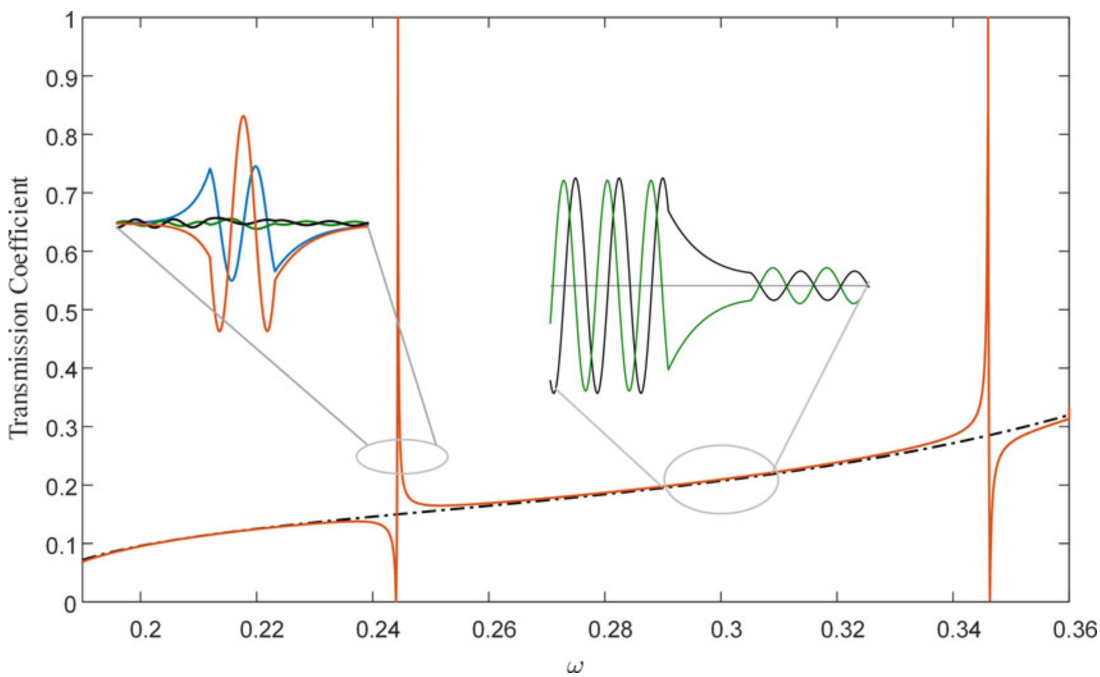

DOI: 10.1109/JPHOT.2017.2782742
1943-0655

Resonances in Bianisotropic Layers

Faroq Razzaz and Majeed A. S. Alkanhal

Department of Electrical Engineering, King Saud University, Riyadh 11421, Saudi Arabia

DOI:10.1109/JPHOT.2017.2782742

Manuscript received October 15, 2017; revised December 1, 2017; accepted December 8, 2017. Date of publication December 18, 2017; date of current version January 3, 2018. This work was supported in part by the College of Engineering Research Center and in part by the Deanship of Scientific Research at King Saud University, Riyadh, Saudi Arabia. Corresponding author: Faroq Razzaz (e-mail: fqaseem@ksu.edu.sa1).

Abstract: This paper rigorously studies the resonant transmission of electromagnetic waves around embedded trapped modes in bianisotropic films and derives the dispersion relations, the embedded mode condition, and the coupling and tunneling of the evanescent wave within the reciprocal lossless bianisotropic layer. The Berreman's matrix model has been developed to obtain the transmission characteristics through the bianisotropic film. When the layer structure was perturbed, a resonance phenomenon was perceived around the distinct trapped modes; these resonances lead to anomalous transmission and field amplifications around the trapped mode frequencies. The parameters of the magnetoelectric tensors can be used to control the number of the trapped modes and accordingly the resonances in the bianisotropic layer material.

Index Terms: Anomalous transmission, bianisotropic layers, resonances, trapped modes.

1. Introduction

The fast developments in contemporary material technology mean that vast attentiveness is paid to the study of the interactions between optical and electromagnetic (EM) fields with complex materials. The general bianisotropic model can electromagnetically represent any general linear complex material and there is magnetoelectric cross coupling between the magnetic and electric fields in such a media model. As a result of their general electromagnetic properties, bianisotropic synthesized materials are studied to potentially develop innovative applications and devices for microwaves, millimeter waves, and terahertz (THz) technologies as in waveguides, wave absorbers, and polarization transformers [1]–[6].

The propagation of EM waves in bianisotropic media was investigated in several studies [2], [3], [7]–[10]. Angular selective transmission can be achieved when an incident wave from a vacuum on a bianisotropic medium results from the existence of an ordinary and an inverted critical angle [11]. Bianisotropic materials can support the propagation of circularly polarized plane waves over a fixed axis if necessary conditions in the constitutive parameters are satisfied [12]. The transmission and reflection coefficients of thin bianisotropic layers can be approximated using the averaging procedure of the second-order impedance boundary conditions at the interfaces [13]. A generalized exponential matrix technique is used to determine the transmission and reflection characteristics of the bianisotropic bounded structure [14] and the chain-matrix algorithm is used to determine the transmission and reflection characteristics of a bounded structure made of different bianisotropic materials [15]. The constitutive parameters of homogeneous bianisotropic medium can be recovered using scattering parameters in one propagation direction [16], while the constitutive parameters of

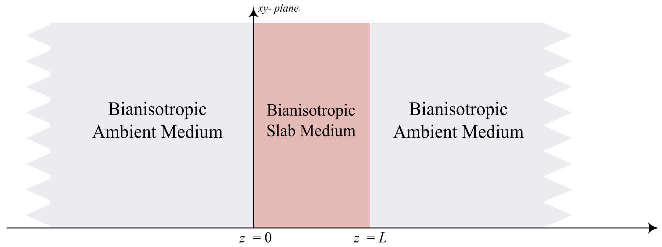

Fig. 1. The problem's physical geometry.

inhomogeneous bianisotropic media can be retrieved using co- and cross-polarized transmission and reflection characteristics [17]. Moreover, the constitutive parameters of biaxial bianisotropic media can be recovered using the state-space method [18]. The polarization behavior of a plane wave that propagates in a reciprocal transversely uniaxial bianisotropic medium perpendicular to the symmetry axis is studied in [19]. Under certain conditions, the transverse electric (TE) and the transverse magnetic (TM) fields can be decoupled independent of the direction of propagation in bianisotropic media [20]. Inhomogeneous bianisotropic materials can be used in the design of both radiating and transferring components in microwave and millimeter wave bands [21].

Several studies on bianisotropic media relevant to the THz band are presented as in [22]–[24]. The control of polarization-rotation for THz and far-infrared waves in bianisotropic media were discussed in [22], [23]. Irregular EM wave propagation in transverse and axial uniaxial bianisotropic media occurs in certain conditions on the media's constitutive parameters [25], [26]; this irregular propagation is characterized by four normally propagating modes and two suppressed modes. Another type of anomalous EM wave propagation that is described by axial Voigt waves can occur in helical bianisotropic media [27] and similar wave behavior is described in optical and EM periodic waveguiding structures [28]–[30]. Several optoelectronics and photonics applications can utilize these EM waves, such as in photonic devices, polarization control and filtering, surface plasmon resonance, and when tuning light emitting diodes and lasers [30].

This work explores the propagating and evanescent wave coupling and tunneling around a bianisotropic layer. It analytically formulates the conditions of discrete trapped mode realization, the resonances around these trapped modes, and associated anomalous transmission and field amplification in an infinite reciprocal lossless bianisotropic film-layer placed in a bianisotropic ambient medium. Berreman's matrix technique is developed to model the transmission characteristics in both resonant and non-resonant states, and the effects of the magnetoelectric parameters on the number of possible trapped modes and the according resonances around the trapped modes are also studied. Furthermore, the instantaneous in-plane field components are presented to show the field amplifications around the trapped mode frequencies in the resonant state.

2. Formulations and Analysis

Studying the evanescent and the propagating waves around the bianisotropic slab/layer requires considering the geometry model presented in Fig. 1, where a reciprocal lossless bianisotropic layer is surrounded by a reciprocal lossless bianisotropic medium. Both the bianisotropic ambient medium and slab/layer are considered to support both evanescent and propagating modes simultaneously at the same frequency and parallel wavevector. The bianisotropic medium can be characterized using the following frequency domain constitutive relationships

$$\bar{D} = \bar{\bar{\varepsilon}}\bar{E} + \bar{\bar{\xi}}\bar{H}$$
$$\bar{B} = \bar{\bar{\xi}}\,\bar{E} + \bar{\bar{\mu}}\bar{H} \tag{1}$$

where $\bar{\bar{\varepsilon}}$, $\bar{\bar{\mu}}$, and $\bar{\bar{\xi}}$ and $\bar{\zeta}$ are the 3×3 permittivity, permeability, and magnetoelectric tensors, respectively.

This study considers a general oblique incident plane wave using time dependency $e^{-i\omega t}$. The EM fields are given by

$$\mathbf{E}\ (x, y, z; t) = \mathbf{E}_0\, e^{i\left(k_x x + k_y y + k_z z - \omega t\right)} = \begin{bmatrix} E_x(z) \\ E_y(z) \\ E_z(z) \end{bmatrix} e^{i\left(k_x x + k_y y - \omega t\right)} \tag{2a}$$

$$\mathbf{H}\ (x, y, z; t) = \mathbf{H}_0\, e^{i\left(k_x x + k_y y + k_z z - \omega t\right)} = \begin{bmatrix} H_x(z) \\ H_y(z) \\ H_z(z) \end{bmatrix} e^{i\left(k_x x + k_y y - \omega t\right)} \tag{2b}$$

where $\kappa = (k_x, k_y)$ is the parallel wavevector to the bianisotropic material and ω is the incident plane wave's frequency. A reduction of the Maxwell equations to a system of four first-order ordinary differential equations for the tangential fields can be obtained using the Berreman 4×4 matrix representation [31].

$$\frac{d\Psi(z)}{dz} = iJA\,\Psi(z) \tag{3}$$

where A is the 4×4 matrix that depends on the permittivity, permeability, magnetoelectric tensors ($\bar{\bar{\varepsilon}}$, $\bar{\bar{\mu}}$, $\bar{\bar{\xi}}$, and $\bar{\bar{\zeta}}$) of the medium, the frequency of the incident wave, and the parallel wavevector components.

Moreover, $\Psi(z)$ and J are respectively defined by

$$\Psi(\mathrm{z}) = \begin{bmatrix} E_x(z) \\ E_y(z) \\ H_x(z) \\ H_y(z) \end{bmatrix} \text{ and } J = \begin{bmatrix} 0 & 0 & 0 & 1 \\ 0 & 0 & -1 & 0 \\ 0 & -1 & 0 & 0 \\ 1 & 0 & 0 & 0 \end{bmatrix}.$$

Consider a reciprocal lossless bianisotropic medium with the following properties:

$$\bar{\bar{\varepsilon}} = \begin{bmatrix} \varepsilon_x & 0 & 0 \\ 0 & \varepsilon_y & 0 \\ 0 & 0 & \varepsilon_z \end{bmatrix},\ \bar{\bar{\mu}} = \begin{bmatrix} \mu_x & 0 & 0 \\ 0 & \mu_y & 0 \\ 0 & 0 & \mu_z \end{bmatrix},$$

$$\bar{\bar{\xi}} = i\begin{bmatrix} 0 & \xi_1 & 0 \\ -\xi_1 & 0 & \xi_2 \\ 0 & -\xi_2 & 0 \end{bmatrix},\ \text{and } \bar{\bar{\zeta}} = \bar{\bar{\xi}} = i\begin{bmatrix} 0 & \xi_1 & 0 \\ -\xi_1 & 0 & \xi_2 \\ 0 & -\xi_2 & 0 \end{bmatrix}.$$

where the magnetoelectric tensors have zero diagonal elements. This can be realized by embedding microstructure omega-shaped conductive particles with specified orientation in an isotropic host matrix [32]–[34]. These properties are carefully chosen to give two propagating and two evanescent modes that correspond to the real and imaginary eigenvalues of the medium matrix iJA of the bianisotropic medium. These eigenvalues are the wavenumbers in the bianisotropic medium in the direction of wave propagation. Hence, the z-directional wavevector components in the bianisotropic medium when $k_y = 0$ are given by

$$k_1 = -k_2 = \sqrt{\varepsilon_x\left(\frac{\omega^2}{c^2}\mu_y - \frac{k_x^2}{\varepsilon_z}\right) - \frac{\omega^2}{c^2}\left(\frac{\varepsilon_x}{\varepsilon_z}\xi_2^2 + \xi_1^2\right)} \tag{4}$$

$$k_3 = -k_4 = \sqrt{\mu_x\left(\frac{\omega^2}{c^2}\varepsilon_y - \frac{k_x^2}{\mu_z}\right) - \frac{\omega^2}{c^2}\left(\frac{\mu_x}{\mu_z}\xi_2^2 + \xi_1^2\right)} \tag{5}$$

where c is the speed of light in a vacuum. The resultant tangential eigenfields associated with these wavenumbers (eigenvalues) are given by

$$v_1^{\pm} = \begin{bmatrix} \pm k_1 - i\frac{\omega}{c}\xi_1 \\ 0 \\ 0 \\ \frac{\omega}{c}\varepsilon_x \end{bmatrix} \tag{6}$$

$$v_3^{\pm} = \begin{bmatrix} 0 \\ \pm k_3 - i\frac{\omega}{c}\xi_1 \\ \frac{k_x^2+\frac{\omega^2}{c^2}\left(\xi_2^2-\varepsilon_y\mu_z\right)}{\frac{\omega}{c}\varepsilon_x} \\ 0 \end{bmatrix} \tag{7}$$

where $v_1^{\pm}$ and $v_3^{\pm}$ denote the positive or negative eigenfields that correspond to the z-directional wavenumbers $\pm k_1$ and $\pm k_3$ respectively.

We studied the evanescent and propagating wave transformation through the bianisotropic interface by adopting that the z-directional wavenumbers ($\pm k_1$) signify an evanescent field in the ambient medium and a propagating field in the slab, while the z-directional wavenumbers ($\pm k_3$) signify a propagating field in the ambient medium and an evanescent field in the slab. Thus, a bianisotropic ambient and layer media that supports these two modes simultaneously requires that the elements of the permittivity, permeability, and magnetoelectric tensors satisfy the following conditions for the ambient and layer media:

$$\frac{\mu_{xa}\varepsilon_{ya} - \frac{\mu_{xa}}{\mu_{za}}\xi_{2a}^2 - \xi_{1a}^2}{\frac{\mu_{xa}}{\mu_{za}}} > \frac{\varepsilon_{xa}\mu_{ya} - \frac{\varepsilon_{xa}}{\varepsilon_{za}}\xi_{2a}^2 - \xi_{1a}^2}{\frac{\varepsilon_{xa}}{\varepsilon_{za}}} \tag{8}$$

$$\frac{\mu_{xs}\varepsilon_{ys} - \frac{\mu_{xs}}{\mu_{zs}}\xi_{2s}^2 - \xi_{1s}^2}{\frac{\mu_{xs}}{\mu_{zs}}} < \frac{\varepsilon_{xs}\mu_{ys} - \frac{\varepsilon_{xs}}{\varepsilon_{zs}}\xi_{2s}^2 - \xi_{1s}^2}{\frac{\varepsilon_{xs}}{\varepsilon_{zs}}} \tag{9}$$

where "a" and "s" refer to the ambient and slab/layer, respectively. Henceforth, the term k_z^{ae} represents the evanescent z-directional wavenumber in the bianisotropic ambient medium and k_z^{sp} represents the propagating z-directional wavenumber in the bianisotropic layer medium. Likewise, the associated evanescent and propagating eigenfields in the ambient medium are represented by $v_{\pm}^{me}$ and $v_{\pm}^{mp}$, respectively, where m denotes the selected medium ("a" or "s").

The trapped modes in the bianisotropic layer can be constructed by matching the propagating fields in the bianisotropic slab with the evanescent fields in the bianisotropic ambient medium. The obtained trapped modes have frequencies that belong to a continual interval I restricted by the dispersion of the evanescent and propagating z-directional wavenumbers in the bianisotropic layer, given by (4) and (5) respectively; i.e.,

$$\sqrt{\left(\frac{\varepsilon_{xs}}{\varepsilon_{zs}}\right) / \left(\varepsilon_{xs}\mu_{ys} - \left(\frac{\varepsilon_{xs}}{\varepsilon_{zs}}\xi_{2s}^2 + \xi_{1s}^2\right)\right)}k_x \le I \le \sqrt{\left(\frac{\mu_{xs}}{\mu_{zs}}\right) / \left(\mu_{xs}\varepsilon_{ys} - \left(\frac{\mu_{xs}}{\mu_{zs}}\xi_{2s}^2 + \xi_{1s}^2\right)\right)}k_x.$$

The coupling of the evanescent wave appears when the frequency of the incident field belongs to the continual frequency interval I and the tangential evanescent waves in the bianisotropic ambient medium match the propagating waves in the bianisotropic layer. A perturbation in the parallel wavevector ($k_y \neq 0$) of the incident wave means that resonances will rise around the trapped modes frequency. However, the propagating fields in the bianisotropic ambient will tunnel across the bianisotropic layer to the other side using the evanescent fields in the bianisotropic layer; this phenomenon is identical to particle tunneling in quantum mechanics.

The fields inside and outside the bianisotropic layer are given by

$$\psi(z) = \begin{cases} C_1 v_-^{ae} e^{-ik_z^{ae} z}, & z < 0 \\ C_2 v_+^{sp} e^{ik_z^{sp} z} + C_3 v_-^{sp} e^{-ik_z^{sp} z}, & 0 < z < L \\ C_4 v_+^{ae} e^{ik_z^{ae}(z-d)}, & z > L \end{cases} \tag{10}$$

Equivalently;

$$\begin{aligned} \begin{bmatrix} E_x \\ E_y \\ H_x \\ H_y \end{bmatrix} &= C_1 \begin{bmatrix} -k_z^{ae} - i\frac{\omega}{c}\xi_{1a} \\ 0 \\ 0 \\ \frac{\omega}{c}\varepsilon_{xa} \end{bmatrix} e^{-ik_z^{ae} z} && (z < 0) \\ &= C_2 \begin{bmatrix} k_z^{sp} - i\frac{\omega}{c}\xi_{1s} \\ 0 \\ 0 \\ \frac{\omega}{c}\varepsilon_{xs} \end{bmatrix} e^{ik_z^{sp} z} + C_3 \begin{bmatrix} -k_z^{sp} - i\frac{\omega}{c}\xi_{1s} \\ 0 \\ 0 \\ \frac{\omega}{c}\varepsilon_{xs} \end{bmatrix} e^{-ik_z^{sp} z} && (0 < z < L) \\ &= C_4 \begin{bmatrix} k_z^{ae} - i\frac{\omega}{c}\xi_{1a} \\ 0 \\ 0 \\ \frac{\omega}{c}\varepsilon_{xa} \end{bmatrix} e^{ik_z^{ae}(z-L)} && (z > L) \end{aligned} \tag{11}$$

The unknown constants C_1, C_2, C_3, and C_4 can be found by applying appropriate boundary conditions. The tangential fields at the boundaries ($z = 0$ and $z = L$) are continuous, then

$$\begin{bmatrix} \left(-k_z^{ae} - i\frac{\omega}{c}\xi_{1a}\right) & -\left(k_z^{sp} - i\frac{\omega}{c}\xi_{1s}\right) & -\left(-k_z^{sp} - i\frac{\omega}{c}\xi_{1s}\right) & 0 \\ \varepsilon_{xa} & -\varepsilon_{xs} & -\varepsilon_{xs} & 0 \\ 0 & \left(k_z^{sp} - i\frac{\omega}{c}\xi_{1s}\right) e^{ik_z^{sp} L} & \left(-k_z^{sp} - i\frac{\omega}{c}\xi_{1s}\right) e^{-ik_z^{sp} L} & -\left(k_z^{ae} - i\frac{\omega}{c}\xi_{1a}\right) \\ 0 & \varepsilon_{xs} e^{ik_z^{sp} L} & \varepsilon_{xs} e^{-ik_z^{sp} L} & -\varepsilon_{xa} \end{bmatrix} \begin{bmatrix} C_1 \\ C_2 \\ C_3 \\ C_4 \end{bmatrix} = 0 \tag{12}$$

For the above system to have a nontrivial solution, the determinant of the matrix must equal zero, then the trapped modes condition is given by

$$2\cos\left(k_z^{sp} L\right) - i\frac{\sin\left(k_3^{sp} L\right)}{\left(\varepsilon_{xa}\varepsilon_{xs} k_z^{ae} k_z^{sp}\right)} \left(\varepsilon_{xs}^2 \left(k_z^{ae}\right)^2 + \varepsilon_{xa}^2 \left(k_z^{sp}\right)^2 + \frac{\omega^2}{c^2}\left(\varepsilon_{xa}\xi_{1s} + \varepsilon_{xs}\xi_{1a}\right)^2\right) = 0 \tag{13}$$

For an incident electromagnetic field on the bianisotropic layer (at $z = 0$), part of this field will be transmitted through the bianisotropic layer and the remainder will be reflected; therefore, the total fields in the ambient medium can be given as:

$$\psi(z) = \begin{cases} v_+^{ap} e^{ik_z^{ap} z} + r_-^p\ v_-^{ap} e^{-ik_z^{ap} z} + r_-^e\ v_-^{ae} e^{-ik_z^{ae} z} & (z < 0) \\ t_+^p\ v_+^{ap}\ e^{ik_z^{ap}(z-L)} + t_+^e\ v_+^{ae}\ e^{ik_z^{ae}(z-L)} & (z > L) \end{cases} \tag{14}$$

where $v_+^{ap} e^{ik_z^{ap} z}$ is the incident field, $v_\pm^{ap,e}$ are the eigenvectors of the eigenvalues $\pm k_z^{ap,e}$, $t_+^{p,e}$ is the magnitude of the transmitted fields and $r_-^{p,e}$ is the magnitude of the reflected fields. The field in the bianisotropic layer can be determined using the transfer matrix [31]

$$\psi(L) = T(0, L)\,\psi(0) \tag{15}$$

$$t_+^p\ v_+^{ap} + t_+^e\ v_+^{ae} = T(0, L)\left(v_+^{ap} + r_-^p\ v_-^{ap} + r_-^e\ v_-^{ae}\right) \tag{16}$$

The matrix $T(0, L) = e^{jJA_s L}$ is the transfer matrix and A_s is the 4×4 matrix that describes the properties of the bianisotropic layer. The reflection and transmission characteristics are found directly from (16).

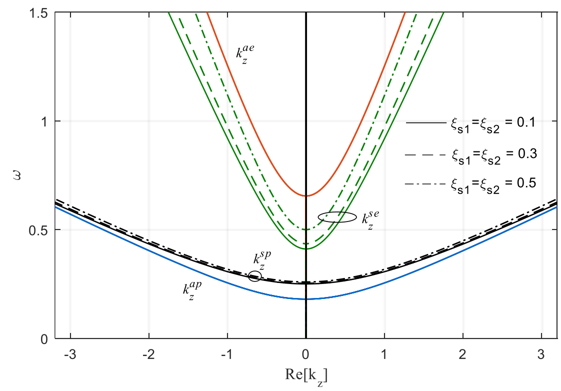

(a)

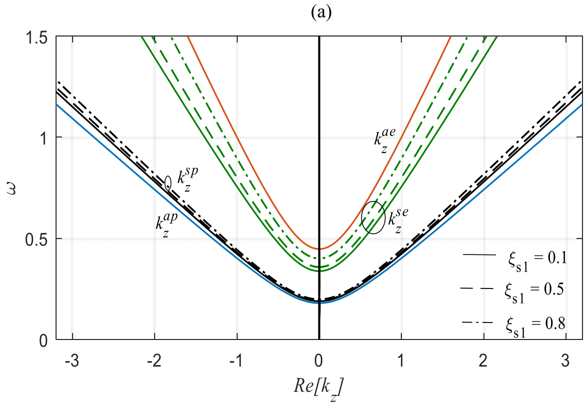

(b)

Fig. 2. The dispersion relations: (a) biaxial bianisotropic layers, (b) uniaxial bianisotropic layers. The red and blue curves represent the *z*-directional evanescent and propagating wavenumbers in the bianisotropic ambient medium, respectively. The green and black curves represent the *z*-directional evanescent and propagating wavenumbers in the bianisotropic layer, respectively, for three different values of magnetoelectric parameters. The continual interval I is restricted by the black and green curves.

3. Results and Discussions

The preceding developed analytical formulations will be used to investigate the behavior of electromagnetic field coupling and tunneling through bianisotropic layers. Dispersion relations, the condition of the modes, resonant and non-resonant transmission characteristics, and anomalies around the trapped mode frequencies of the reciprocal lossless bianisotropic layer will be discussed.

In this section, two bianisotropic arrangements are considered to validate the developed analytical formulations. The first arrangement is with biaxial bianisotropic media and the second arrangement is with uniaxial bianisotropic media. For the biaxial bianisotropic media, the properties of the ambient medium are selected as $\varepsilon_{xa} = 1.5,\ \varepsilon_{ya} = 8,\ \varepsilon_{za} = 1,\ \mu_{xa} = 4,\ \mu_{ya} = 1,\ \mu_{za} = 1$, and $\xi_{1a} = \xi_{2a} = 0.5$. Additionally, the properties of the slab/layer medium are selected such that $\varepsilon_{xs} = 8,\ \varepsilon_{ys} = 1.5,\ \varepsilon_{zs} = 1,\ \mu_{xs} = 1,\ \mu_{ys} = 4,\ \mu_{zs} = 1$, and the magnetoelectric tensor elements are given by $\xi_{1s} = \xi_{2s} = 0.1,\ 0.3$, and 0.5. For the uniaxial bianisotropic media, the properties are selected as $\varepsilon_{xa} = 1.5,\ \varepsilon_{ya} = 8,\ \varepsilon_{za} = 1.5,\ \mu_{xa} = 1,\ \mu_{ya} = 1,\ \mu_{za} = 1,\ \xi_{1a} = 0.5$, and $\xi_{2a} = 0$, for the ambient media and $\varepsilon_{xs} = 7,\ \varepsilon_{ys} = 2.2,\ \varepsilon_{zs} = 7,\ \mu_{xs} = 1,\ \mu_{ys} = 1,\ \mu_{zs} = 1$ with the magnetoelectric tensor elements given by $\xi_{1s} = 0.1,\ 0.3$, and 0.5 and $\xi_{2s} = 0$, for the film. These properties of the media are selected to satisfy the prescribed conditions (8) and (9). In such structures, two distinct propagating and evanescent wavenumbers are conceivable in each medium.

The dispersion relations between the angular frequency and the real *z*-directional wavenumber are as depicted in Fig. 2. The continuum frequency interval I is shown in Fig. 2 bounded by the propagating and evanescent *z*-directional wavenumber in the bianisotropic layer. This continual

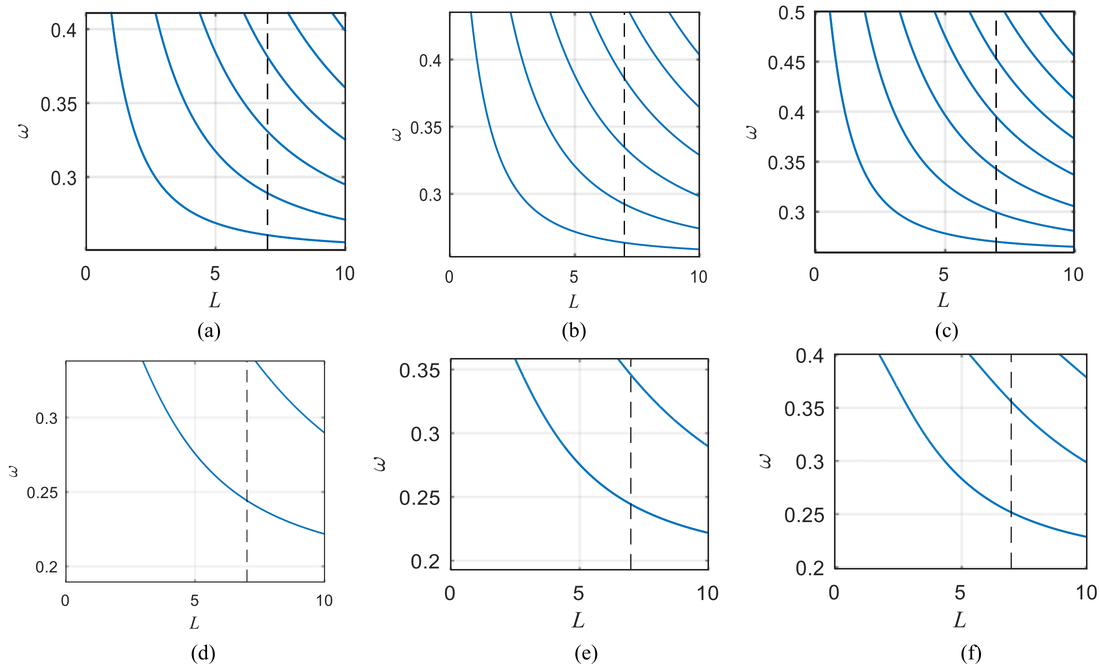

Fig. 3. Trapped modes: (a) biaxial bianisotropic $\xi_{1s} = \xi_{2s} = 0.1$, (b) biaxial bianisotropic $\xi_{1s} = \xi_{2s} = 0.3$, (c) biaxial bianisotropic $\xi_{1s} = \xi_{2s} = 0.5$, (d) uniaxial bianisotropic $\xi_{1s} = 0.1$, (e) uniaxial bianisotropic $\xi_{1s} = 0.5$, and (f) uniaxial bianisotropic $\xi_{1s} = 0.8$.

Table 1
Frequencies of Trapped Modes in the Biaxial Structure

$\xi_{1s} = \xi_{2s}$		0.1	0.3	0.5
I		[0.250352, 0.410997]	[0.253225, 0.435194]	[0.259281, 0.500000]
Trapped Modes Frequencies	**Mode 0**	0.260570	0.263568	0.269872
	Mode 1	0.288988	0.292336	0.299328
	Mode 2	0.330773	0.334638	0.342629
	Mode 3	0.381365	0.385849	0.395017
	Mode 4	—	—	0.453115

interval I extends (and consequently the number of the conceivable trapped modes) as the values of ξ_{1s} and ξ_{2s} increase. For example, in biaxial layers, when $\xi_{1s} = \xi_{2s} = 0.1$ and 0.3, there are four trapped modes, whereas there are five trapped modes when $\xi_{1s} = \xi_{2s} = 0.5$ for the layer thickness ($L = 7$ unit length), as depicted in Fig. 3. The uniaxial film supports fewer trapped modes. For example, there is one mode when $\xi_{1s} = 0.1$ and two trapped when $\xi_{1s} = 0.5$ or 0.8 when L = 7 unit length. Each mode line characterizes a conceivable trapped mode and their frequencies for the layer thickness L. When the parallel wavevector set to $\kappa = (k_x, k_y) = (0.5, 0)$, the obtained trapped modes are perfect and decoupled from the radiation mode in the ambient medium. However, these trapped modes are unsteady or non-robust for perturbation of the parallel wavevector ($ky \neq 0$).

Table 2
Frequencies of Trapped Modes in the Uniaxial Structure

ξ_{1s}		0.1	0.5	0.8
I		[0.189117, 0.337868]	[0.192450, 0.358050]	[0.198262, 0.400320]
Trapped Modes Frequencies	**Mode 0**	0.239610	0.244003	0.251364
	Mode 1	———	0.345657	0.355634

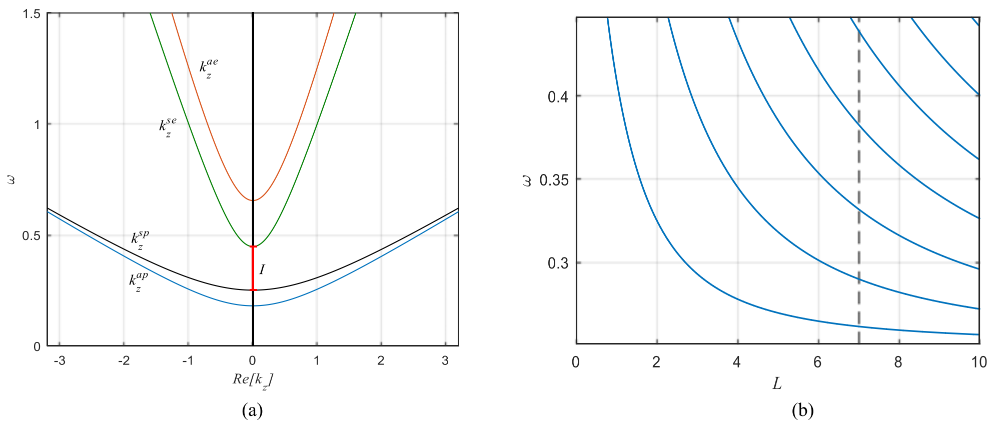

Fig. 4. (a) Dispersion relations when $\xi_{1s} = 0.5$ and $\xi_{2s} = 0$, and (b) trapped modes when $\xi_{1s} = 0.5$ and $\xi_{2s} = 0$.

Tables 1 and 2 summarize the width of the band I, the number of trapped modes embedded in the continual interval I, and their frequencies for three different values of magnetoelectric parameters for the biaxial and uniaxial arrangements, respectively. Another case that can be tested here is when $\xi_{2s} = 0$ while ξ_{1s} varies. Here, the band I again extends as the value of ξ_{1s} increases. When $\xi_{1s} = 0.5$, I is located at frequencies in the range 0.250982–0.447213 with five trapped modes that are supported by this slab, as shown in Fig. 4. These trapped modes are placed at $\omega = 0.262251,\ 0.289821,\ 0.331854,\ 0.382765$, and 0.439307. The last case examined here is when $\xi_{1s} = 0$ and ξ_{2s} vary. Band I also increases as the value of ξ_{1s} increases (when $\xi_{2s} = 0.8$, band I will extend from 0.272772 to 0.539163); there are six trapped modes supported by the slab, as shown in Fig. 5. The frequencies of these trapped modes are $\omega = 0.283837,\ 0.314563,\ 0.359616,\ 0.413968,\ 0.474300$, and 0.537884. Furthermore, the number of trapped modes and their frequencies can be effectively controlled by the thickness of the bianisotropic layer. Likewise, for the uniaxial structure, the frequencies of the trapped modes in the film are listed in Table 2.

The transmission coefficients for the biaxial and uniaxial structures with different magnetoelectric parameters are traced in Fig. 6. When the parallel components of the wavevector of the incident plane wave are set to $\kappa = (k_x,\ k_y) = (0.5,\ 0)$, the bianisotropic layer admits all perfect trapped modes (dash-dot black lines in Fig. 6). However, when the parallel wavevector is perturbed to $\kappa = (0.5,\ 0.03)$, resonances arise around the frequencies of the ensuing non-robust trapped modes. Resonances are represented by sharp transmission anomalies (totally transmitted and totally reflected) with intense field amplification.

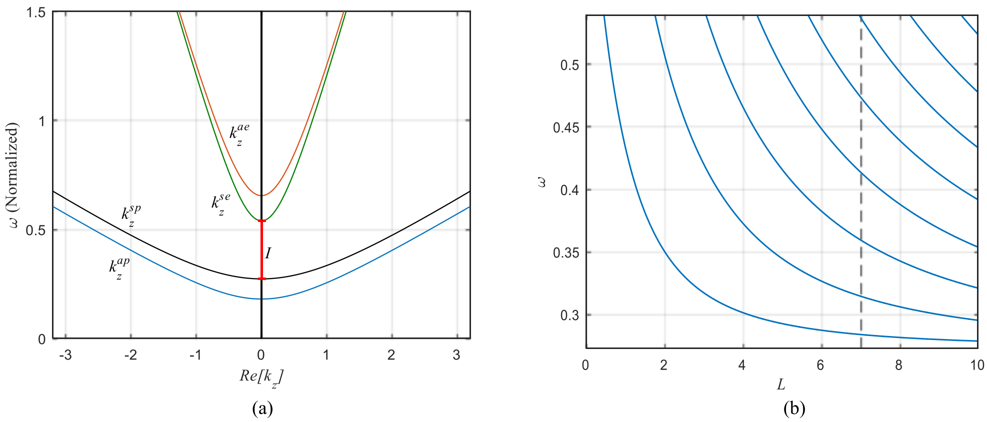

Fig. 5. (a) Dispersion relations when $\xi_{1s} = 0$ and $\xi_{2s} = 0.8$, and (b) trapped modes when $\xi_{1s} = 0$ and $\xi_{2s} = 0.8$.

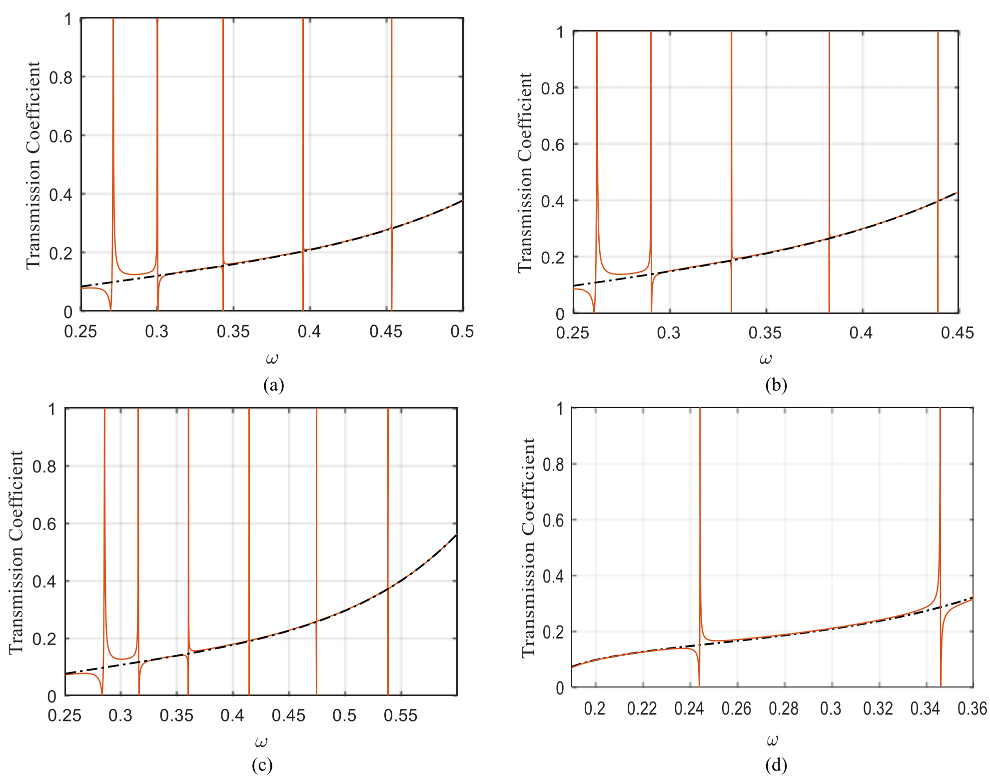

Fig. 6. Transmission coefficient: (a) biaxial bianisotropic layers; $\xi_{1s} = 0.5$ and $\xi_{2s} = 0.1$, (b) biaxial layers; $\xi_{1s} = 0.5$ and $\xi_{2s} = 0$, (c) biaxial media; $\xi_{1s} = 0$ and $\xi_{2s} = 0.8$, and (d) uniaxial bianisotropic layers; $\xi_{1s} = 0.5$. (The dashed black line represents $\kappa = (0.5,\ 0.0)$ and the red line represents $\kappa = (0.5,\ 0.03)$).

Fig. 7(a) shows the tangential fields distribution (E_x and H_y) in the biaxial bianisotropic media at trapped mode frequency $\omega = 0.330773$ (mode 2) when $\xi_{1s} = \xi_{2s} = 0.1$ and $L = 7$. When an incident perturbed propagating field with a frequency near a perfect trapped mode hits the biaxial bianisotropic interface, the fields within the bianisotropic layer are highly amplified and the trapped modes resemble Fig. 7(b). This figure shows the fields distribution in the structure at resonance $\kappa = (0.5,\ 0.03)$, $\xi_{1s} = \xi_{2s} = 0.1$, and $\omega = 0.331145$. Fig. 7(c) shows the tangential fields (E_x and H_y) at frequency $\omega = 0.251364$ (mode 0) when $\xi_{1s} = 0.8$ and $L = 7$ in the uniaxial layers. When an incident perturbed propagating field with a frequency near a perfect trapped mode hits the

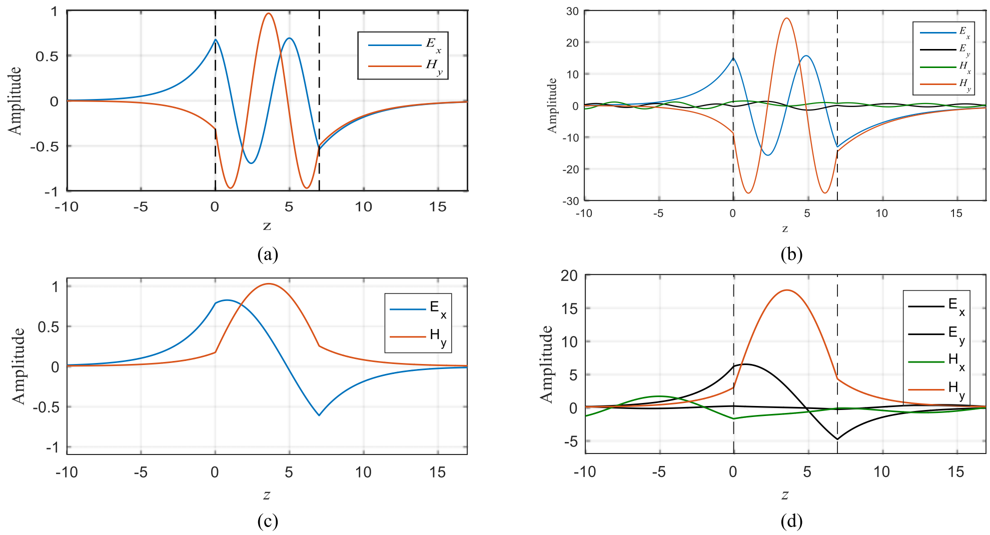

Fig. 7. Transverse field distribution: (a) biaxial bianisotropic layers ($\xi_{1s} = \xi_{2s} = 0.1$ and $L = 7$) at trapped mode $\omega = 0.330773$ and $\kappa = (0.5,\ 0)$, (b) biaxial bianisotropic layers at resonance $\omega = 0.331145$ and $\kappa = (0.5,\ 0.03)$, (c) uniaxial bianisotropic layers ($\xi_{1s} = 0.8$ and $L = 7$) at trapped mode $\omega = 0.251364$ and $\kappa = (0.5,\ 0)$, and (d) uniaxial layers at resonance $\omega = 0.251686$ and $\kappa = (0.5,\ 0.03)$.

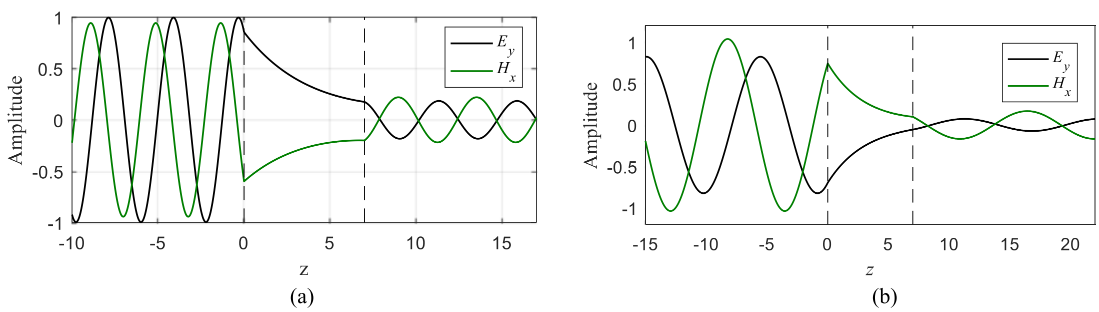

Fig. 8. Tunneling of the field across the film: (a) biaxial bianisotropic layers at $\omega = 0.35$ and (b) uniaxial bianisotropic layers at $\omega = 0.30$.

uniaxial film interface, the fields within the film are highly amplified and the trapped modes resemble Fig. 7(d). This figure depicts the fields in the structure at resonance $\kappa = (0.5,\ 0.03)$, $\xi_{1s} = 0.8$, and $\omega = 0.251626$.

Furthermore, Fig. 8 shows the field distribution when the incident-propagating plane wave in the ambient medium is tunneled by means of the evanescent field through the bianisotropic interface. As mentioned above, the frequency of the incident wave ($\omega = 0.35$ for the biaxial structure and $\omega = 0.30$ for the uniaxial structure) has to be within the continuous spectral interval I.

4. Conclusion

This paper contains an analytical exploration of electromagnetic tunneling, coupling, and resonances in bianisotropic films. The characterization of the physical conditions for evanescent field tunneling and coupling through a reciprocal lossless bianisotropic layer is thoroughly studied and formulated and mathematical models are established for the number of the possible trapped modes in the bianisotropic layer and their frequencies. The values and directions of the magnetoelectric parameters have a noticeable impact on the frequencies of the trapped modes and on the width of the continual band where the trapped modes are entrenched. Field resonances characterized by sharp anomalous reflection/transmission and with intense field amplification in the bianisotropic layer are verified as arising when the parallel wavevector of the incident wave is perturbed with a frequency near the frequency of the trapped mode. Electromagnetic wave tunneling through evanescent waves in the slab can be derived if the incident field frequency belongs to the continual frequency interval of the material layer. The results obtained in this research are valuable in the bianisotropic thin film coating characterization of THz, optical, and sub-optical applications.

Acknowledgment

The authors acknowledge the administrative support of this research from the College of Engineering Research Center and the Deanship of Scientific Research at King Saud University, Riyadh, Saudi Arabia.

References

[1] W.-Y. Yin, L.-W. Li, O. Ooi, P.-S. Kooi, and M. Leong, "Interaction of EM waves with bianisotropic objects: Clarification of magnetic symmetry groups," in *Proc. Antennas Propag. Soc. Int. Symp., 2001*, 2001, pp. 200–203.
[2] I. O. Vardiambasis, J. Tsalamengas, and K. Kostogiannis, "Propagation of EM waves in composite bianisotropic cylindrical structures," *IEEE Trans. Microw. Theory Techn.*, vol. 51, no. 3, pp. 761–766, Mar. 2003.
[3] S. Rikte, G. Kristensson, and M. Andersson, "Propagation in bianisotropic media-reflection and transmission," *IEE Proc. Microw., Antennas Propag.*, vol. 148, pp. 29–36, 2001.
[4] C. E. Kriegler, M. S. Rill, S. Linden, and M. Wegener, "Bianisotropic photonic metamaterials," *IEEE J. Sel. Topics Quantum Electron.*, vol. 16, no. 2, pp. 367–375, Mar./Apr. 2010.
[5] F. Bilotti, L. Vegni, and A. Alu, "U-patch antenna loaded by complex substrates for multifrequency operation," *Microw. Opt. Technol. Lett.*, vol. 32, pp. 3–5, 2002.
[6] S.-Y. Wang, W.-Y. Yin, L. Zhou, J. Chen, X.-Q. Gu, and L.-F. Qiu, "THz wave interaction with planar structures consisting of multilayer graphene sheets and bianisotropic slabs," in *Proc. IEEE Int. Wireless Symp.*, 2014, pp. 1–4.
[7] I. V. Lindell, A. J. Viitanen, and P. K. Kolvisto, "Plane-wave propagation in a transversely bianisotropic uniaxial medium," *Microw. Opt. Technol. Lett.*, vol. 6, pp. 478–481, 1993.
[8] I. V. Lindell and A. J. Viitanen, "Plane wave propagation in uniaxial bianisotropic medium," *Electron. Lett.*, vol. 29, pp. 150–152, 1993.
[9] S. M. Keller and G. P. Carman, "Electromagnetic wave propagation in (bianisotropic) magnetoelectric materials," *J. Intell. Mater. Syst. Struct.*, vol. 24, pp. 651–668, 2013.
[10] U. C. Hasar, J. J. Barroso, Y. Kaya, T. Karacali, and M. Ertugrul, "Investigation of transmitted, reflected, and absorbed powers of periodic and aperiodic multilayered structures composed of bi-anisotropic metamaterial slab and conventional material," *Photon. Nanostruct.-Fundam. Appl.*, vol. 13, pp. 106–119, 2015.
[11] P.-H. Chang, C.-Y. Kuo, and R.-L. Chern, "Wave propagation in bianisotropic metamaterials: Angular selective transmission," *Opt. Express*, vol. 22, pp. 25710–25721, 2014.
[12] A. Lakhtakia, "Conditions for circularly polarized plane wave propagation in a linear bianisotropic medium," *Electromagnetics*, vol. 22, pp. 123–127, 2002.
[13] D. Khaliullin and S. Tretyakov, "Reflection and transmission coefficients for thin bianisotropic layers," *IEE Proc. Microw., Antennas Propag.*, vol. 145, pp. 163–168, 1998.
[14] W.-Y. Yin and L.-W. Li, "Reflection and transmission characteristics of bianisotropic," *Microw. Opt. Technol. Lett.*, vol. 21, pp. 351–356, 1999.
[15] R. D. Graglia, P. L. Uslenghi, and R. E. Zich, "Reflection and transmission for planar structures of bianisotropic media," *Electromagnetics*, vol. 11, pp. 193–208, 1991.
[16] Z. Li, K. Aydin, and E. Ozbay, "Determination of the effective constitutive parameters of bianisotropic metamaterials from reflection and transmission coefficients," *Phys. Rev. E*, vol. 79, 2009, Art. no. 026610.
[17] A. Farahbakhsh, D. Zarifi, A. Abdolali, and M. Soleimani, "Technique for inversion of an inhomogeneous bianisotropic slab through an optimisation approach," *IET Microw. Antennas Propag.*, vol. 7, pp. 436–443, 2013.
[18] D. Zarifi, M. Soleimani, and A. Abdolali, "Electromagnetic characterization of biaxial bianisotropic media using the state space approach," *IEEE Trans. Antennas Propag.*, vol. 62, no. 3, pp. 1538–1542, Mar. 2014.
[19] X. Cheng, J. A. Kong, and L. Ran, "Polarization of waves in reciprocal and nonreciprocal uniaxially bianisotropic media," *PIERS Online*, vol. 4, pp. 331–335, 2008.
[20] P. L. Uslenghi, "TE-TM decoupling for guided propagation in bianisotropic media," *IEEE Trans. Antennas Propag.*, vol. 45, no. 2, pp. 284–286, Feb. 1997.
[21] A. Toscano, L. Vegni, and F. Bilotti, "Inhomogeneous bianisotropic materials for antenna and circuit applications in microwave and millimetre wave ranges," Dept. of Electron. Eng., , Roma Tre University, Rome, Italy, DTIC Document2000.
[22] G. Kenanakis, E. N. Economou, C. M. Soukoulis, and M. Kafesaki, "Controlling THz and far-IR waves with chiral and bianisotropic metamaterials," *EPJ Appl. Metamaterials*, vol. 2, p. 15, 2015.
[23] S. Yu-Lei, Z. Qing-Li, L. Wei, Z. Dong-Mei, L. Lei, and Z. Cun-Lin, "Terahertz wave polarization rotation in bianisotropic metamaterials," *Chin. Phys. B*, vol. 20, 2011, Art. no. 094102.
[24] X.-l. Xu, B.-G. Quan, C.-Z. Gu, and L. Wang, "Bianisotropic response of microfabricated metamaterials in the terahertz region," *J. Opt. Soc. Amer. B*, vol. 23, pp. 1174–1180, 2006.
[25] W. Weiglhofer, "On anomalous propagation in axially uniaxial bianisotropic mediums," *Int. J. Infrared Millim. Waves*, vol. 20, pp. 1277–1286, 1999.

[26] W. Weiglhofer, “On anomalous propagation in transversely uniaxial bianisotropic mediums,” *Int. J. Infrared Millim. Waves*, vol. 21, pp. 895–904, 2000.
[27] A. Lakhtakia, “Anomalous axial propagation in helicoidal bianisotropic media,” *Opt. Commun.*, vol. 157, pp. 193–201, 1998.
[28] S. Shipman, “Resonant scattering by open periodic waveguides,” *Progress Prog. Comput. Phys.*, vol. 1, pp. 7–49, 2010.
[29] S. Fan and J. Joannopoulos, “Analysis of guided resonances in photonic crystal slabs,” *Phys. Rev. B*, vol. 65, 2002, Art. no. 235112.
[30] S. P. Shipman, J. Ribbeck, K. H. Smith, and C. Weeks, “A discrete model for resonance near embedded bound states,” *IEEE Photon. J.*, vol. 2, no. 6, pp. 911–923, Dec. 2010.
[31] D. W. Berreman, “Optics in stratified and anisotropic media: 4 $\times$ 4-matrix formulation,” *J. Opt. Soc. Amer.*, vol. 62, pp. 502–510, 1972.
[32] H. Hatefi-Ardakani and J. Rashed-Mohassel, “Study of mode propagation in pseudochiral transmission lines,” *Prog. Electromagn. Res. M*, vol. 10, pp. 39–47, 2009.
[33] S. Tretyakov, A. Sihvola, A. Sochava, and C. Simovski, “Magnetoelectric interactions in bi-anisotropic media,” *J. Electromagn. Waves Appl.*, vol. 12, pp. 481–497, 1998.
[34] A. Sochava, C. Simovski, and S. Tretyakov, “Chiral effects and eigenwaves in bi-anisotropic omega structures,” in *Advances in Complex Electromagnetic Materials*. New York, NY, USA: Springer, 1997, pp. 85–102.